

**COMPUTATIONAL FLUID DYNAMICS ANALYSIS OF MOISTURE
INGRESS IN AIRCRAFT STRUCTURAL COMPOSITE MATERIALS**O. Anwar Bég¹, Bettina Islam^{2**}, MD. Shamshuddin^{3*}, Tasveer A. Bég⁴¹*Aeronautical & Mechanical Engineering Department, School of Computing, Science and Engineering, Newton Building, University of Salford, Manchester, M54WT, UK.**Email: O.A.Beg@salford.ac.uk*²*School of Mechanical, Aerospace and Civil Engineering, The University of Manchester, George Begg Building, Manchester, M13 9PL, UK.**Email: bettyislam1993aero@gmail.com*³*Department of Mathematics, Vaagdevi College of Engineering, Warangal, Telangana, India.**Email: shammaths@gmail.com*⁴*Computational Mechanics and Dynamics Research, Israfil House, Dickenson Rd., Manchester, M13, UK.**Email: tasveerabeg@gmail.com***Corresponding author: Email- shamshuddin_md@vaagdevi.edu.in****Now at ENVISA- 71-73, Rue Des Denouettes, 75015, Paris, FRANCE***ABSTRACT**

Moisture in composite materials has been proven to be an important issue leading to significant deterioration of commercial aircraft wing structures. Lingering problems associated with this issue which is initiated with defects during manufacturing and finishing include delamination, de-bonding, potential fracture, debris etc. Despite extensive investigation and refinement in structural design, the water ingress problem persists as no general mitigation technique has yet been developed. Developing sustainable solutions to the water ingress problem can be very time-consuming and costly. The increasing use of composites in the aviation industry, in, for example, honeycomb sandwich components highlights the significant need to address the moisture ingress problem and develop deeper insights which can assist in combatting this problem. Experimental testing, although the most dependable approach, can take months, if not years. Numerical simulations provide a powerful and alternative approach to experimental studies for obtaining an insight into the mechanisms and impact of moisture ingress in aircraft composites. The principal advantage is that they can be conducted considerably faster, are less costly than laboratory testing, and furthermore can also utilize the results of laboratory studies to aid in visualizing practical problems. Therefore, the present study applies a computational fluid dynamics (CFD) methodology, specifically ANSYS finite volume software and the three fluid-based solvers, Fluent, CFX and ANSYS fluid structure interaction (FSI), to simulate water ingress in composite aerospace structures. It is demonstrated that ANSYS Fluent is a satisfactory computational solver for fundamental studies, providing reasonably accurate results relatively quickly, especially while simulating two-dimensional components. Three-dimensional components are ideally simulated on CFX, although the accuracy achievable is reduced. The structural-fluid based solver, ANSYS FSI (fluid structure interaction), unfortunately does not fully implement the material studied leading to reduced accuracy. The simulations reveal interesting features associated with different inlet velocities, inlet fastener hole numbers, void number and dimensions. Pressure, velocity, streamline, total deformation and normal stress plots are presented with extensive interpretation. Furthermore, some possible mitigation pathways for water ingress effects including hydrophobic coatings are outlined.

KEY WORDS: Aircraft composites, Computational Fluid Dynamics, ANSYS, moisture ingress, Fluent, CFX, (fluid structure interaction) FSI, velocity, pressure, total deformation; elevator, mesh density.

NOMENCLATURE

\bar{F}	external body force vector (N)
\bar{g}	gravity vector (m/s ²)
I	identity matrix in FLUENT for isotropic mass diffusivity of water
p	static pressure (Pa)
N	number of scalar equations in FLUENT mass transfer (Fickian species diffusion) model
S_m	user-defined source (water species)
s_{ϕ_k}	source term in “user-defined” species model
t	time (s)
u_i	velocity vector for species conservation equation
\bar{v}	velocity vector (u, v, w components in the x, y, z coordinate directions)
V	inlet velocity for CFD mesh (m/s)
x_i	Cartesian coordinates (x, y, z),

GREEK

μ	dynamic viscosity of water (kgm/s)
ρ	fluid density (kg/m ³)
ϕ_k	species (water)
Γ_k	general tensor form for anisotropic diffusion
$\Gamma_k I$	isotropic mass diffusivity of the water (m ² /s)
$\bar{\tau}$	stress tensor in Navier-Stokes equations
∇	3-D Laplacian operator

ABBREVIATIONS:

ADINA	Automatic Dynamic Incremental Nonlinear Analysis (MIT multi-physics finite element code)
CFD	Computational Fluid Dynamics
CFRP	Carbon Fiber Reinforced Polymers
NACA	National Advisory Committee for Aeronautics
NDT	Non-Destructive Testing

1. INTRODUCTION

The world of aerospace is changing. Composite materials are infiltrating into many areas of flight technology. First deployed in military aircraft in the 1960s, composite materials were utilized in commercial aircraft much later in the 1980s. The key advantage to the military industry was the improvement of speed and maneuverability. The later adoption of composites in civil aviation is attributable to the stringent airworthiness requirements and the flat price of fuel in the late 1980s for which fuel efficiency was not necessary. Composites were considered as revolutionary materials complimenting and replacing the traditional metallic alloy structural materials used for many decades in commercial aerospace. The Airbus A380 was the first aircraft to use composite materials as the primary load-carrying structure, especially in its wings, which achieved a significant reduction of fuel consumption of up to 17% per passenger compared with other similar airliners. Progressively modern commercial aircraft are increasingly embracing new composites including primary loaded carbon fiber reinforced materials. With this scale of use of composites, it is critical to identify and correct any weakness of these materials to avoid worst case scenarios. With increasing numbers of commercial aircraft in use, greenhouse gas emissions harmful to the environment abounding and other industrial emissions, lower fuel consumption is an ideal solution, and this is better achieved with lighter (composite) aircraft structures. This is integral to the global thrust towards a greener planet for current and future generations. A composite material essentially consists of two components, fibers and matrix. This leads to a final product which possesses superior structural properties than the individual components. Fibers are strong in tension but weak in compression. Stiffness is achieved from the matrix structure which however is able to hold its shape and can continuously be fabricated. Aircraft structural components are generally featuring ever-increasing percentages of composite materials.

Different types of fibers and matrix exist, and each combination leads to unique material properties. Aramid fibers or Kevlar fibers are aromatic polyamide fibers, defined by low density, high strength and modulus, damage resistance. They are used for ballistic protection, cables and also as reinforcement for plastics in automotive, aerospace and marine technologies. Glass fiber reinforcement is the most commonly used and the lowest in cost being commonly featured in roof insulation, piping, automobile chassis designs and even medical equipment. This is largely due to the ease of fabrication, high strength-to-weight ratio and good resistance to heat. The fibers of most importance for the aerospace industry are glass fibers. Carbon Fiber Reinforced Polymers (CRFPs) are also very popular. CFRP components have excellent fatigue and damage tolerance properties. The Airbus A380 uses CFRP in the horizontal and vertical tail plane, elevators, rudder, belly fairing, upper deck floor beams, main landing gear doors, flaps, spoilers and ailerons.

The maintenance of composite structures under real environmental loadings as elaborated earlier is critical. The principal reason for water ingress is the presence of any sort of defect in the composite materials. This particular product always requires a careful, judicious and flawless fabrication. Any factor of lesser quality or mistake could lead to defects, which will have significant drawbacks to the materials, as elaborated by Anderson and Altan [1]. Hayes and Gammon [2] reported that several factors influence the quantity and location of voids such as curing parameters, thickness of the material, compaction pressure, surface morphology, fiber bridging and excessive resin bleed. Numerous aircraft parts which are made of composites such as elevators, rudders or wings are set with hundreds of rivets and fasteners, which imply many holes. Any minor maintenance error can result in loose fasteners, thus creating a path for moisture to penetrate the material especially at high temperature and pressure variations. Wong and Tamin [3] quite recently identified the major mechanisms of moisture sorption in polymeric

composites. Mechanical properties of the composite structural aircraft component are likely to be strongly affected by moisture and timely rectification is essential in avoiding potentially catastrophic failures. The first observable effect is an increase in weight of the component due to absorption of water.

Extensive experimental studies have been conducted to study water ingress in real composite components in both the aircraft and marine industries for over four decades. Although the source of water in marine applications is seawater, and that in aircraft is due to rain and de-icing, many similar characteristics in material response over time have been identified. Very early studies of water ingress in aero-composites include the seminal article of Mazor et al., [4] in which results of an 11-year real time study (1965-1977) for the influence of water ingress on carbon-epoxy and graphite-epoxy composites were presented, using carefully controlled US Naval Ordnance Laboratory ring samples. Moisture desorption tests were reported, and weight gain and mass diffusion coefficients evaluated. Furthermore, this study presented a range of horizontal shear and flexural tests were performed on both “wet” and partially and completely dried specimens (for residual properties) and demonstrated that flexural composite strength is unaffected via exposure whereas shear strength of the carbon-epoxy composites experiences significant degradation. Once a material has been exposed to water ingress, it is more prone to absorb water and eventually becomes weakened through softening of the resin, swelling and loss of mechanical performance. Water or other fluids such as kerosene, de-icing agents or hydraulic fluid promote nose bond failure and induce composite layer delamination and skin disbanding. Marom and Broutman [5] examined water ingress in both glass fiber and graphite fiber-reinforced epoxies for both stressed and unstressed materials, observing that the imposition of external stresses and greater angle between the loading and fiber directions both elevate the rate of moisture absorption, maximum moisture content and furthermore enhances diffusion coefficients. Further studies in the context of rotary-wing honeycomb composites have been communicated by Jackson and O’Brien [6] and for aircraft wings by Komai [7] Cise and Lakes [8]. LaPlante [9] has applied magnetic resonance (MR) imaging as a non-destructive testing (NDT) method for quantifying water penetration in honeycomb composite sandwich panels. He considered ingress into both the structural panel and the bonding adhesive itself and noted the superiority of this approach in establishing accurately et al., the spatial distribution of moisture within materials. Crawley [10] described the degradation of helicopter structural panels under fluid penetration with non-destructive testing (NDT) methods. Li et al., [11] addressed both water penetration and subsequent percolation within airplane rudder composite structures. Arici [12] considered water migration and subsequent hydrothermal aging of polyetherimide composite aero-structural components. Youssef et al., [13] conducted extensive sets of experiments to show the time-dependent nature of water diffusivity in organic matrix composites. Similar studies were presented by Dana et al., [14]. Interfacial degradation and void content influence on composite integrity under water ingress were assessed respectively by [15-16] for a wide spectrum of aero-composites including carbon fiber/epoxy and carbon fiber/bismaleimide composites. These investigations *all confirmed the inherent complexity of the moisture ingress phenomenon in aircraft composite structures* and the considerable concern to both airline operators and maintenance facilities regarding, in particular the *skin-to-core bonding degradation*, which compromises structural integrity and therefore presents a serious safety issue. Many corporations and airliners have sought an easy-to-use and generally applicable method of detecting such ingress and recently vacuum-assisted active thermography has been proposed. However, heating has the undesirable and counter-productive feature of inducing *permanent adhesive degradation* especially under high temperature, long-duration exposure. Ibarra-Castanedo [17] has documented that in a study that involved fifteen Boeing 767 aircraft, it was

found that these aircraft could contain up to 40 kilograms of water, especially in the external honeycomb composite panels. Few solutions exist to remove the water out of a component. However, the most common and effective solution has been a total component replacement which implies a significant maintenance burden and a longer aircraft grounding time.

The multi-scale nature of water ingress dynamics in aero-composites may also be resolved from a different viewpoint- *computational simulation*. In recent years finite element and other computational algorithms (molecular dynamics, smooth particle hydrodynamics, Monte Carlo simulation, finite volume methods, Lattice Boltzmann techniques) and hardware capabilities have progressed massively. This has enabled engineers to simulate multi-scale transport phenomena in geophysical [18], biological [19], chemical [20] etc., in complex geometries with high speed and substantially greater accuracy. Numerical simulation of water ingress into aero-composites, although not addressed to anywhere near the level of these other areas, has also embraced these developments. A number of interesting works have appeared. Ionita [21] used a Voroni cell geometry-based finite element method to analyze the moisture ingress in polymeric foam composite sandwich panels. Gueribiz et al., [22] developed a numerical model for stress-dependent coupled diffusive water ingress in a homogeneous, isotropic polymer matrix composite. Telford et al., [23] employed a finite element model to analyze the moisture ingress in unsymmetric composite laminates, calibrating their model with experimentally measured curvatures and demonstrating that water penetration strongly modifies the through-thickness residual stresses. Vavilov et al., [24] employed both infrared thermography and a 3-dimensional panel model to simulate the water ingress in aircraft honeycomb cells.

The principal objective of the present paper is to investigate using computational fluid dynamics the influence of water ingress on aero-composite structures, motivated by exploring possible pathways for mitigating water ingress and reducing high maintenance costs. The composite has to be simulated as a porous medium to allow ingress of water. Many approaches exist for this including hierarchical porous models, volume-averaging, reconstructed porous media etc. They are lucidly reviewed in [25]. However, to visualize pressure and velocity distributions, commercial finite volume codes provide a fast, relatively inexpensive and powerful strategy. The ANSYS [26] and CFX [27] commercial software is therefore employed with a porosity model. These tools provide a good methodology to simulate the components exposed to water ingress in order to evaluate the damages, high internal stresses and the influence of water diffusivity on composite material structural integrity. Fick's law governing the moisture diffusion process is employed. Mesh-independence is included. A standard elevator composite structure featured in commercial aircraft is selected as the main geometry for the studies. Two-dimensional simulations are performed with ANSYS FLUENT [26]. Three-dimensional analysis is conducted with ANSYS CFX [27] and also different composite materials are examined. Fluid-Structure Interaction (FSI) is also addressed. The computations reveal some interesting features of the water ingress problem and also provide a platform for more refined simulations with alternate methods (e.g. Molecular Dynamics and Direct Simulation Monte Carlo methods).

2. GEOMETRIC AND MATHEMATICAL MODELS

2.1 Geometric Model

A standard elevator featuring in narrow-bodied commercial aircraft is selected as the main geometry for the present simulations, since water ingress has largely been detected in aircraft elevators and rudders [8]. Another

advantage of conducting simulations on elevators is that the shape can be very similar to an aircraft wing and the studies and outcomes can be extended to the topics of wings. A NACA (National Advisory Committee for Aeronautics) 4412 aerofoil geometry which is very commonly deployed for aircraft wings and which resembles greatly an actual elevator is therefore investigated. This aerofoil has a maximum thickness of 12% at 30% chord and a maximum camber of 4% at 40% chord. The dimensions of the elevator chosen were inspired from an Airbus A320F (A318/A319/A320/A321) and are depicted in fig. 1. The most common composite material employed in elevator aero-structures, based on industrial recommendations [28], is the carbon fibre honeycomb composite AS4-3k/E7K8 which is utilized in both commercial and military jet engine aircraft for aerofoils and thrust reverser doors. This is therefore selected for preliminary computations.

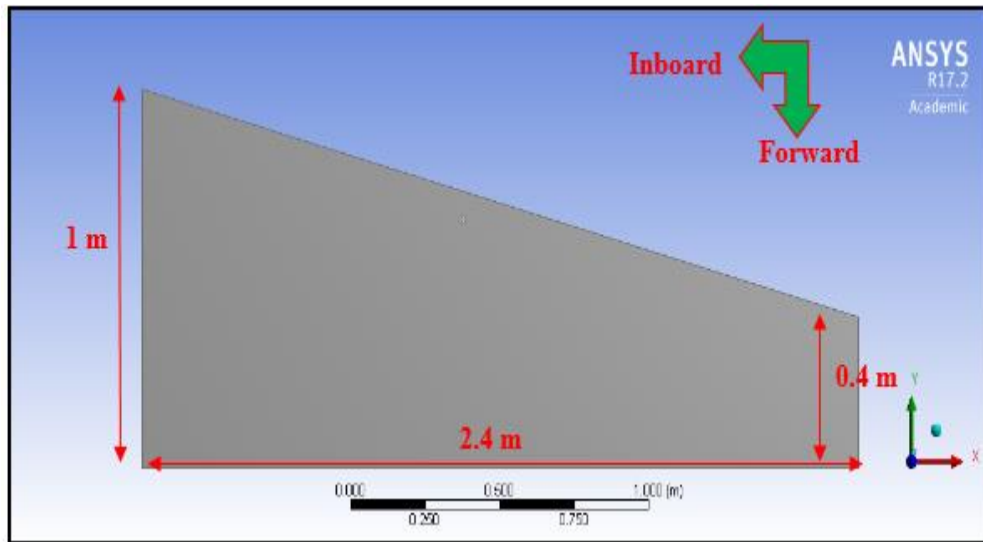


Fig. 1: Upper surface of a standard A320F Elevator used in simulations

2.2 ANSYS FLUENT Flow Model Equations

ANSYS FLUENT [26] is a versatile, finite volume method-based CFD (computational fluid dynamics) code. It utilizes both pressure and density-based solvers for flow computation and allows excellent mesh design for complex geometrical configurations. The water is simulated a Newtonian fluid and constant viscosity and density are considered. In the “material physics” option this is the default setting. The simulation of moisture ingress in composite materials can be conducted by solving the mass, momentum and species conservation equations for a porous medium. The general form of mass conservation equation is used, which is valid for both compressible and incompressible flows. The vector form of the unsteady mass conservation equation is as follows (ANSYS [26]):

$$\frac{\partial \rho}{\partial t} + \nabla \cdot (\rho \vec{v}) = S_m \quad (1)$$

Here ρ is fluid density, t is time, ∇ is the 3-D Laplacian operator, \vec{v} is the velocity vector (u, v, w components in the x, y, z coordinate directions), S_m is any user-defined source and defines the mass added to the continuous phase from the dispersed second phase. The momentum equation is used by the solver to derive the velocity field. The conservation of momentum in an inertial (non-accelerating) reference frame is described by the vector form of the Navier-Stokes equations:

$$\frac{\partial(\rho\bar{v})}{\partial t} + \nabla \cdot (\rho\bar{v}\bar{v}) = -\nabla p + \nabla \cdot (\bar{\tau}) + \rho\bar{g} + \bar{F} \quad (2)$$

Here $\frac{\partial(\rho\bar{v})}{\partial t}$ are the unsteady convective terms, $\nabla \cdot (\rho\bar{v}\bar{v})$ are the spatial nonlinear terms, p is the static pressure,

$\bar{\tau}$ is the stress tensor [26] featuring the *dynamic viscosity* μ , $\rho\bar{g}$, \bar{F} are the gravitational body force and external body force vectors, respectively. It is noteworthy that \bar{F} also contains other model-dependent source terms including magnetic drag, Coriolis forces, porous-media body forces or *Darcian drag* (only the last of these is selected in the current study for the initial analysis). For single-phase mass transfer, for an arbitrary scale (the species is water in this study), ϕ_k , which is employed in due course (for the first simulation), the following equation is solved by ANSYS FLUENT (Islam [29]):

$$\frac{\partial(\rho\phi_k)}{\partial t} + \frac{\partial}{\partial x_i} \left(\rho u_i \phi_k - \Gamma_k \frac{\partial \phi_k}{\partial x_i} \right) = S_{\phi_k} \quad k = 1, 2, \dots, N \quad (3)$$

Here x_i are the coordinates (x, y, z) , u_i is the velocity vector for species, Γ_k and S_{ϕ_k} are respectively the tensor for the general case of anisotropic diffusion and source term which are “user-defined” for each of the N scalar equations. In the present simulations however, isotropic mass diffusivity of the water is assumed and Γ_k in ANSYS FLUENT is therefore defined as $\Gamma_k I$ where I is the identity matrix. ANSYS FLUENT is based on two types of solvers – see [30-31], which are manually selected. These are the pressure-based solver and density-based coupled solver. The pressure-based solvers take the “pressure correction” with velocity and pressure as the primary variables adjusted. Pressure-velocity coupling algorithms are derived by reformatting the aforementioned continuity equation [32]. The pressure-based solver is therefore used for the current simulations. The principal data required for FLUENT simulations is the *composite density*, given as 1560 kg/m^3 . **Tables 1 and 2** give the properties of other materials considered for simulations tests:

Table 1: Epoxy CFRP data

Aerofoil	NACA 4412
Material	Epoxy CFRP 70% Fibres
Material Density	1600 kg/m^3
Top Surface dimensions	Fixed Inner Edge Fuselage: 1 m Length: 2.4 m Outer Edge: 0.4 m

Table 2: Kevlar Aramid Data

Aerofoil	NACA 4412
Material	Kevlar Aramid CFRP
Material Density	1400 kg/m^3
Top Surface dimensions	Fixed Inner Edge Fuselage: 1 m Length: 2.4 m Outer Edge: 0.4 m

2.3 ANSYS FLUENT Pre-Processing

Having gathered the above data, a two-dimensional simulation is initially conducted in the ANSYS Workbench Fluent module in order to visualise the flow path and pressure differences on both the upper surface of the elevator geometry and furthermore along the transverse cross-sectional area. To simulate defects (entry points for water), at the top surface two holes of diameter 1.5cm are inserted on both the leading and trailing edges. The following procedure is repeated for all subsequent 2-D simulations: Having constructed the elevator geometry, based on selected dimensions, the surface area is then produced (Fig. 2). The two holes represent fastener holes on the top surface of an elevator as a mean of water penetration and hence are defined as inlets. The most important part, as mentioned earlier, is then the mesh. A very fine mesh was obtained by inserting the element sizing as 0.006m, as shown in fig. 3. The inlets and the domain are required to be specified, which would allow the setup to be performed in an easier matter as the solver would automatically recognise the fluid inlet and the studied body (fig. 4). The setup follows the mesh. The model is chosen as 'volume of fluid' to allow the material to be defined as porous; the correct material properties is entered for the fluid and the solid material the latter being defined with the component density. Boundary conditions are set with the velocity inlet and surface body. The setup is complete once the input of reference values was done with the flow velocity: the flow commutes from the inlet to the reference zone, the domain. This allows the solver to calculate the solution and provide results in the form of graphical representations. Simulations generated are described in due course.

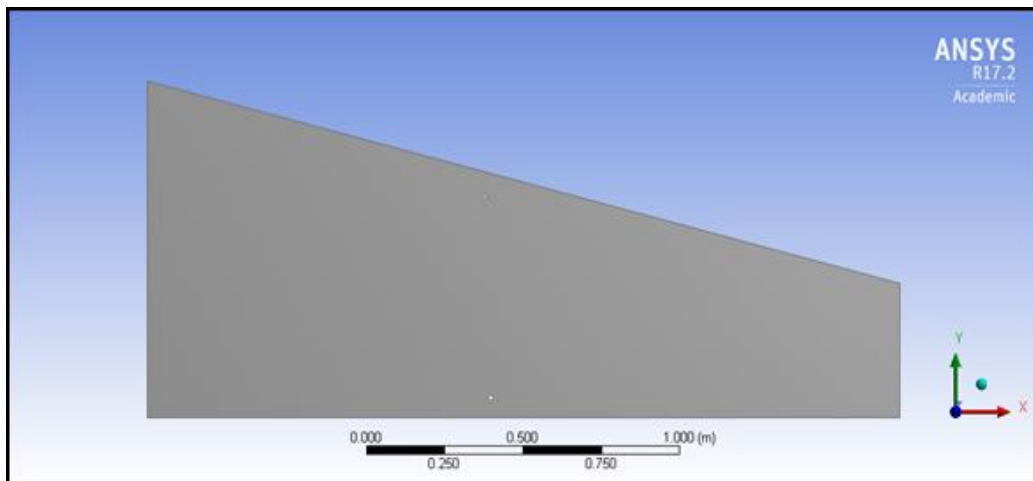


Fig. 2: 2D Simulation Step 1: Geometry - Top Surface with 2 Holes

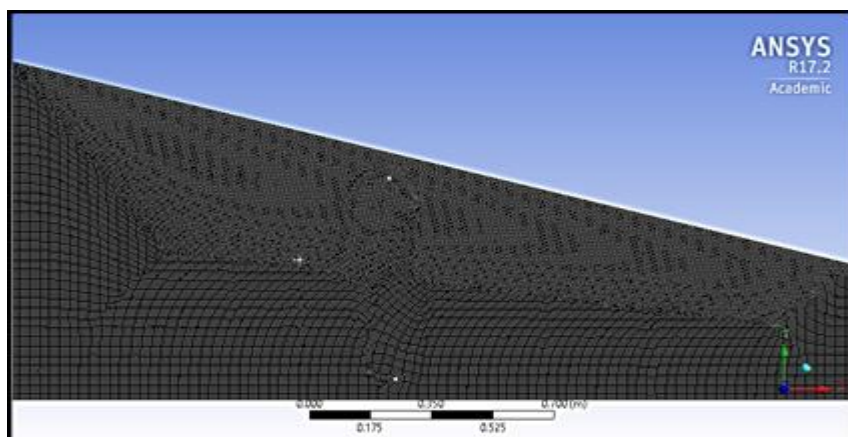


Fig. 3: 2D Simulation Step 2: Fine Mesh

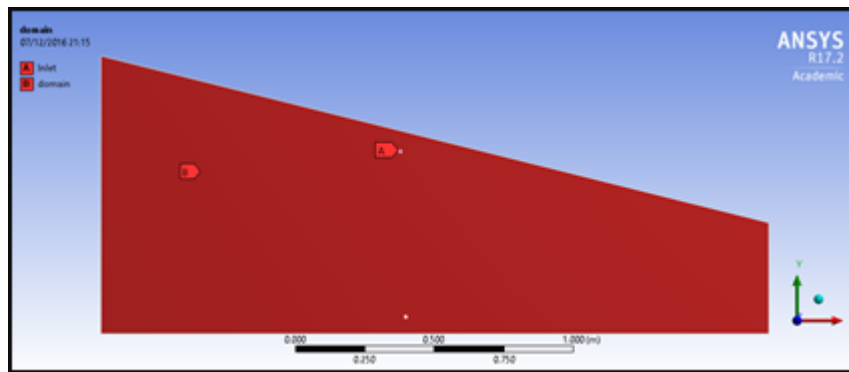


Fig. 4: 2D Simulation Step 2: Mesh + Specification of names

3. CFX AND FSI ANSYS SIMULATIONS

CFX was chosen to conduct 3-dimensional simulations as it allows better visualization of flow paths inside a component (i.e. the porous media model of the elevator). The workspace area is different from ANSYS FLUENT. Nevertheless, the input parameters remain more or less the same. CFX requires clear indication of the domain in the geometry defining the actual region of the fluid flow, with the requisite specification of fluid material type and associated properties (air, water etc) [33]. For CFX, the only changes occur at the setup interface where it is again required to select and enter material properties, correspond the elements/nodes/faces of the materials to the material and/or specific conditions such as density, viscosity etc. Calculated data are required to be entered along with the analysis type; it is also essential to define the fluid ingress, the velocity and other known parameters.

FSI (Fluid Structure Interaction) analysis is also conducted in ANSYS FLUENT. The FSI solver involves the *coupling of the flow field to the deforming structural matrix* and is a part of the *multi-physics options* in ANSYS workbench. Both fluid and structure (composite material) interact in *real time*. The fluid may be internal or external or both. This feature is very useful in many applications including aerospace and also computational biomechanics [34]. The interactions between fluids and structures can be stable or oscillatory. In oscillatory interactions, the strain induced in the solid structure causes it to move such that the source of the strain is reduced, causing the structure to return to its former state, only for the process to repeat. An excellent perspective of FSI (fluid structure interaction) generally is provided by Bathe et al., [35]. As with the CFX solver, the FSI (fluid structure interaction) solver is only different at the set-up interface where loads, supports and constraints must be carefully prescribed by selecting the appropriate geometry, indicating the correct values and directions to obtain accurate simulations. The advantage of the FSI set-up interface is that it also calculates and provides the solution on the same window and is therefore substantially less time-consuming and less expensive compared with Fluent and CFX as these require continuous updating. A new window has to be opened for each mesh, set-up, solution and result page. FSI (fluid structure interaction) therefore achieves significant time-compression.

4. SOLVER COMPARISON AND MESH CONVERGENCE STUDIES

The simulations of moisture ingress in composites with the aid of computational fluid dynamics have not been attempted comprehensively in the scientific literature. A key motivation therefore of the present work is to understand the performance characteristics for the solvers available in the ANSYS suite and the specifications

required to obtain satisfactory simulations. This then allows the proper premise for assessing the quality and accuracy of the results obtained. Considering three dimensional simulations on CFX, this assessment is initially conducted through a *mesh convergence analysis*, in order to obtain a correct value of the element sizing such that the results are close, if not equal, to the desired and expected result.

The preliminary analysis with ANSYS FLUENT is the case study of an elevator composed of epoxy resin with loose fasteners which enables the moisture to penetrate. This case is simulated using different element sizes by refinement until the simulated inlet velocity is closer to the required input inlet velocity of 5 m/s. **Table 3** summarizes the initial CFX mesh results. **Fig. 5 and 6** depict the meshing differences between the original and the quintuple one, illustrating the mesh density increase of 500%. The very fine mesh in Fig. 6 produces much better resolution of the computations but is also more expensive and time consuming. Fig. 7 shows the summary of computations for the simulated velocity against number of elements.

Table 3: Mesh Convergence Initial Study - CFX

Mesh	Element Size (m)	No. of Elements	No. of nodes	Max inlet Velocity as compared to 5m/s	Meshing time (s)	Max Pressure obtained (Pa)	Computational time (minutes)
Original	0.05	14943	3727	4.553	5	22700	5
Double Refinement	0.025	109928	22561	4.537	5.48	26810	6
Triple Refinement	0.016	422541	81602	4.735	13.42	25820	10'30''
Quadruple Refinement	0.0125	873984	162805	4.594	21.69	35430	20'13''
Quintuple Refinement	0.01	1708432	311728	4.613	40.26	35980	45'15''

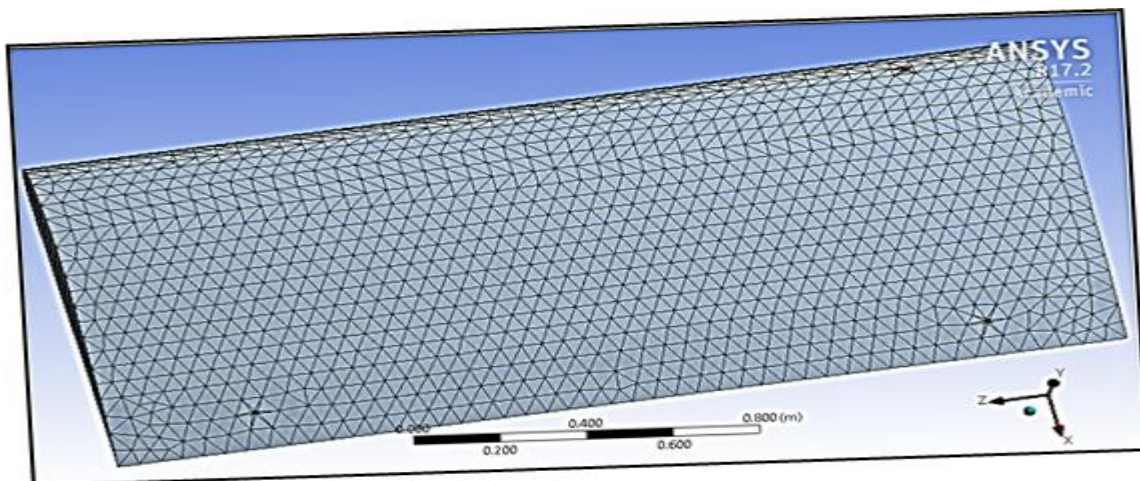


Fig. 5: Mesh sizing: 0.05m - original mesh – CFX

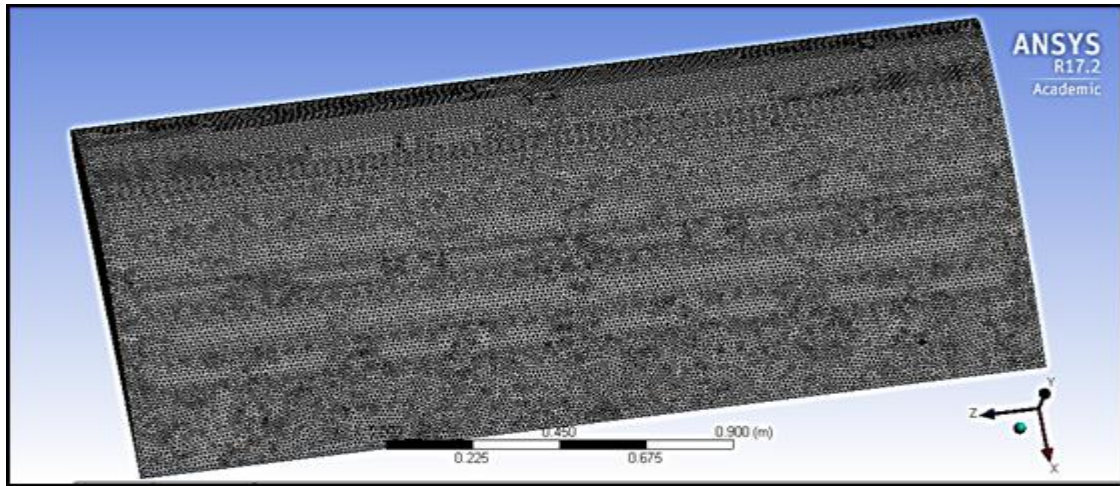


Fig. 6: Mesh sizing: 0.01 – five times greater grid density in refinement - CFX

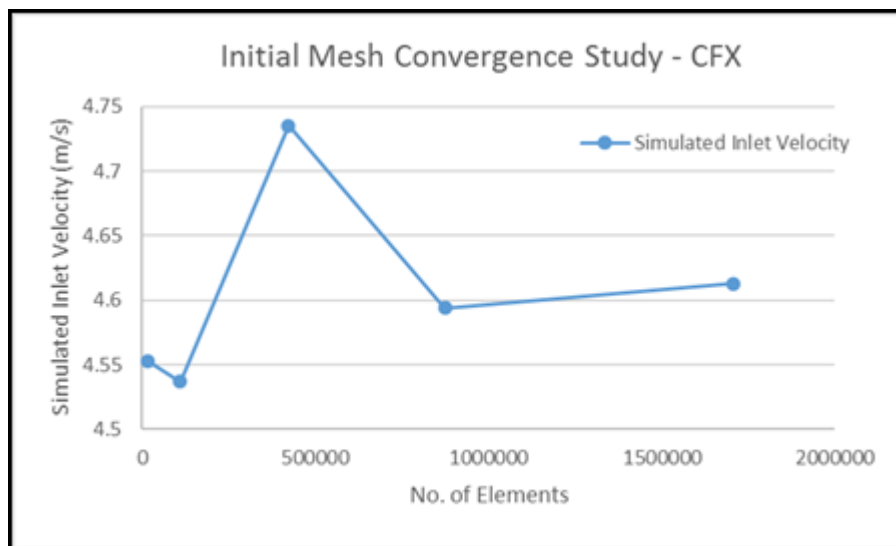


Fig. 7: Simulated Velocity against No. of Elements

An interesting observation is noteworthy. It is customary in numerical analysis that a finer mesh and therefore more elements produce better result which should be closer to the correct solution. However, the above plot shows that accuracy is increased initially but optimized at a critical mesh density. This optimal case corresponds to a mesh with an element size of 0.016 m since this leads to the *highest value of the inlet velocity* being the closest to the desired velocity of 5 m/s. The total computational time for this simulation was 600 s, being relatively quick and did not cause any compilation issues during the solution processing. Therefore, the 3D simulations on CFX are optimized for accuracy with an element mesh of 0.016m. It is noted that these results were obtained with a relatively coarse mesh density, intermediate smoothing and fine angle centre. Of course, amending these specifications to fine and high smoothing would inevitably improve the results. Another possible cause of optimal meshing is attributable to the type of elements used. Zooming into the mesh clearly shows that ANSYS CFX automatically simulates with tetrahedral elements, as illustrated in **Fig. 8**.

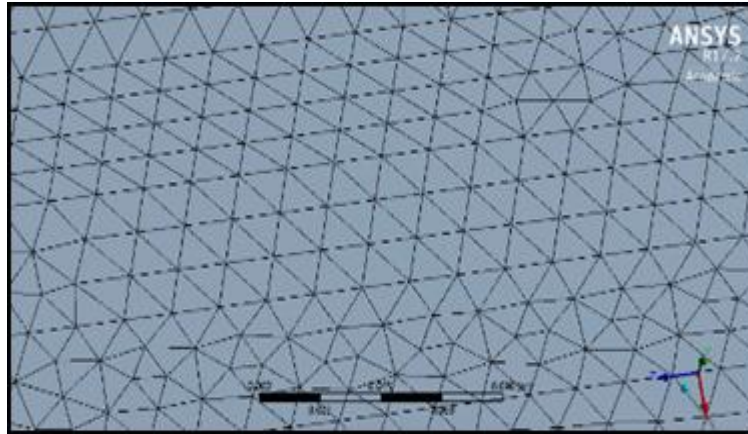


Fig. 8: Tetrahedral elements utilized in CFX

This mesh convergence study is also performed with ANSYS FLUENT to allow a comparison between both CFX and FLUENT solvers. FLUENT has primarily been used as a support to 2-dimensional simulations while CFX as elaborated earlier has been implemented for 3-dimensional analysis. A very similar mesh convergence study is conducted, refining the mesh each time until the inlet velocity value approaches the desired value of 5 m/s. The mesh refinement experiments are summarized in **Table 4**. The quadruple refinement is shown to produce a very satisfactory value of 4.9 m/s of the inlet velocity which eventually converges to the input velocity of 5 m/s.

Table 4: Fluent Mesh Convergence Study

Mesh	Element Size (m)	No. of Elements	No. of nodes	Max inlet Velocity as compared to 5m/s	Meshing time (sec)	Computational time (s)
Original	0.02	4238	4393	2.449	9	60
Double Refinement	0.01	16757	17055	3.963	36	100
Triple Refinement	0.006	46779	47281	4.584	132	150
Quadruple Refinement	0.005	67308	67906	4.9	220	2400

Fig. 9 presents the ANSYS FLUENT mesh convergence study. As anticipated an increasing number of elements increases the accuracy of the results and therefore, generates precise and reliable solutions. An element size of 0.005 m is however numerically time-consuming and therefore the preferred element size of 0.006 m is adopted allowing faster and sufficiently accurate solutions to be obtained. ANSYS FLUENT automatically generates the meshing using quadrilateral elements unlike CFX which defaults to triangular elements. Quadrilateral elements generally yield improved results compared with linear elements which utilize different shape functions. Quadrilateral elements are preferred in finite element modelling within elastic domains, (as in the present study) for which they reduce the approximation error along with the number of elements as compared to triangles. Although triangular meshes remain the simplest polygon in finite element meshing, problems arise when subdividing geometries to increase resolution and when a mesh is to be deformed, as demonstrated through the CFX mesh convergence study. On the other hand, quadrilateral meshes as employed in the ANSYS FLUENT analysis (**Fig. 10**) ensure *clean mesh topology* and therefore guarantee that the model will deform correctly when animated. Therefore, the mesh would have a cleaner appearance unlike a triangular mesh. In the case of smoothing,

triangles would generate anomalies across the surfaces. ANSYS FLUENT achieves higher accuracy with quadrilateral meshes and anomalies can be circumvented.

The mesh generation and refinement study has effectively shown that to simulate water (species) ingress in a composite material, ANSYS FLUENT is preferable for 2-dimensional analysis whereas CFX is a better option for three-dimensional simulations.

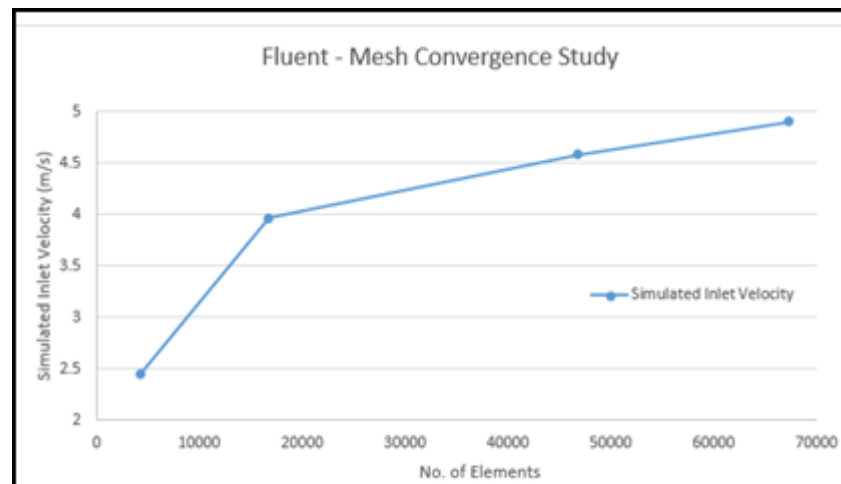


Fig. 9: Fluent - Mesh Convergence Plot

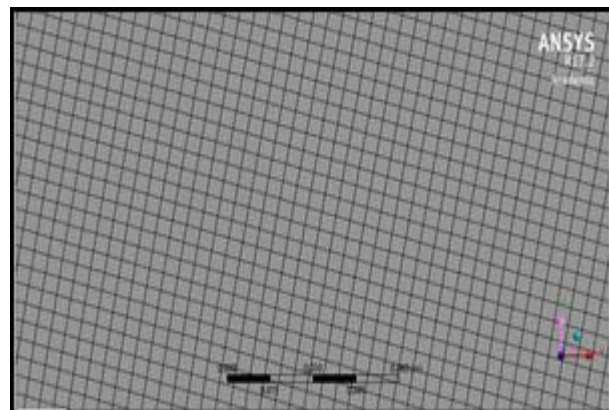


Fig. 10: Quad elements automatically generated by ANSYS Fluent

5. ANSYS AND CFX SIMULATIONS AND RESULTS

In this section we examine the influence of a number of geometric, hydrodynamic and composite material parameters on the pressure and velocity field distributions in the 2-dimensional and 3-dimensional models. Six aspects are considered- *respectively the influence of geometric fastener hole configurations (numbers), water ingress speed, composite body void numbers, void dimensions, whole three-dimensional elevator water ingress (CFX) and finally composite type (CFX results are given for three materials, namely AS4-3k / Carbon Fiber Reinforced Polymers (CFRP) Epoxy / Kevlar)*. The visualizations are depicted in **Figs. 11-27**.

5.1 Effects of increasing affected fastener holes

Figs. 11-13 show the modification in pressure distribution when the number of ingress holes is varied. **Fig. 11** illustrates the first scenario considered- two affected fastener holes show the highest-pressure concentration at the fasteners and non-negligible pressure along the inlet centrelines. Pressure magnitudes decrease radially away from

the inlet holes and merge in the central elevator zone. There is a weaker pressure field generated laterally towards the tip and also in the opposite direction. However, the significant pressure is localized around the inlet zones. **Fig. 12** presents the second scenario- wherein the number of affected holes has been tripled to six. Evidently there is a much wider pressure distribution generated on the top surface of the elevator. Greater pressures (red zones) are also dispersed more and the central elevator zone where the pressure fields meet indicates greater pressures (yellow zone) as compared with fig. 11 (green zone). The migration of water is therefore clearly encouraged with greater numbers of holes and penetrates deeper into the elevator central region. Fig. 13 shows the computed pressure contours with 24 holes (12 distributed at the leading edge and 12 at the trailing edge). Moisture ingress is clearly significantly assisted, and the pressure distributions are dramatically altered. The pressure concentrations around the inlet holes in figs. 11 and 12 are now displaced towards *primarily the leading edge in the vicinity of the elevator tip* (bottom right red zone). In the event of several loose fasteners allowing moisture to enter, non-negligible pressure is seen to be applied by the water on the elevator with higher moisture presence. Lower pressures (darker blue) are now generated at the leftmost zone of the leading edge and also trailing edge with even lower pressures sporadically distributed (darker blue zones) dispersed further into the elevator away from the boundaries. The larger pressure values clearly migrate towards the elevator tip region (yellow and green zones) with the maximum (red zone) magnitudes associated with the outermost tip region. Based on Fick's law of mass diffusion, increasing the number of inlets clearly encourages mass migration (species diffusion) from areas of high-water concentration (inlets) to areas of lower concentration within the composite matrix. Higher pressures experienced at the inlet zones with fewer holes are however modified to a *skewed pressure distribution* towards the elevator tip edge. Highest pressure is therefore only sustained at and around the inlets when they are relatively low in number. The mass transfer (ingress) process is considerably transformed with larger numbers of holes. In this latter case, the implication is that higher pressure is concentrated in a smaller area, which could manifest in significant loss in mechanical strength due to the moisture accumulation in this specific location. The increased weight could also generate larger moments about the body edge (left most boundary of the elevator) leading to structural instability. Without doubt overall, the quantity of inlet holes exerts a profound impact on the species (water) ingress and associated pressure field distribution.

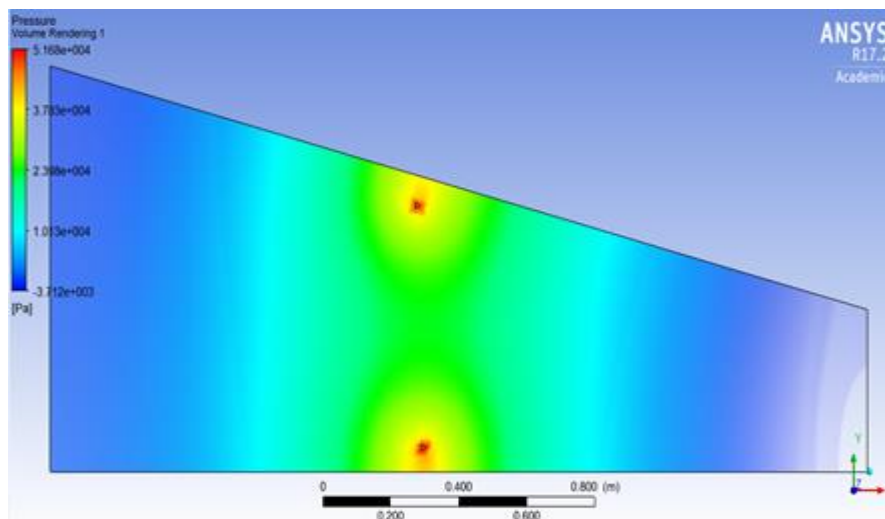


Fig. 11: 2 affected fastener holes - top surface - pressure contour

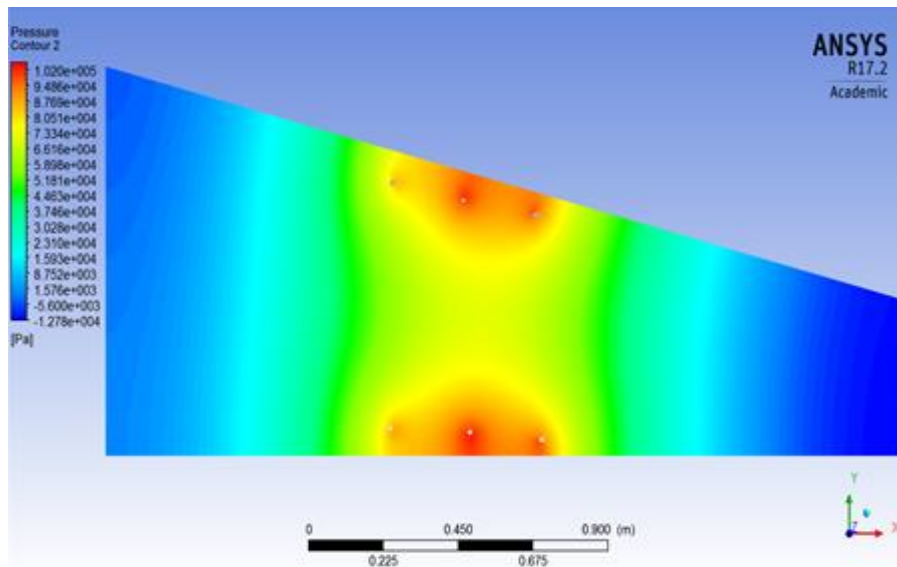


Fig. 12: 6 affected fastener holes - top surface - pressure contour

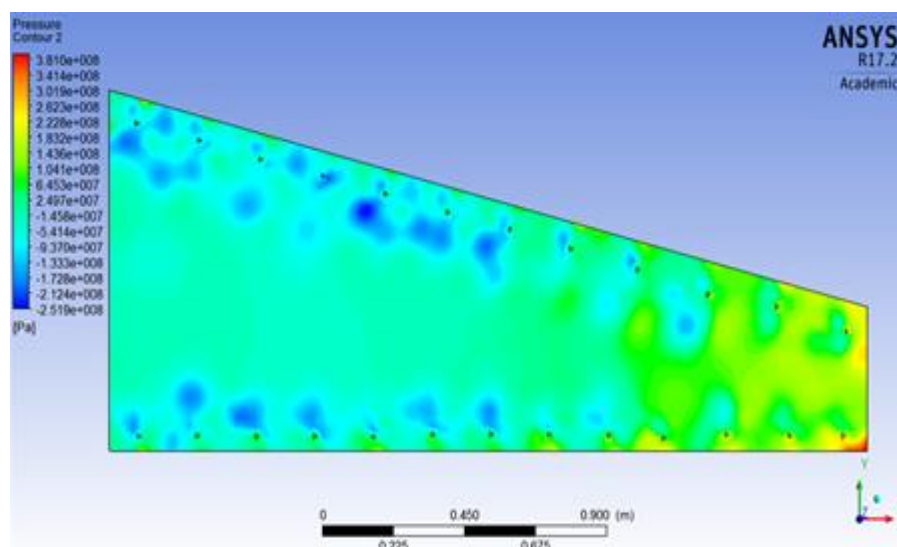


Fig. 13: 24 affected fastener holes - top surface - pressure contour

5.2 Effects of increasing water ingress speed

Regarding the influence of moisture velocity, **Figs. 14-16**, aim to mimic inflight conditions. Most commercial airliners cruise at transonic speeds and flight velocities will exceed Mach 0.7 i.e. 230 m/s. Ingress velocities of course will not approach anywhere near these magnitudes. Based on experimental studies - see refs. [10-20] an estimate range of 5m/s to 100m/s appears feasible. Fig. 14 shows that at an inlet speed of 5 m/s, the moisture is seen to be mainly present around the inlets, with the highest velocity at the inlets. Velocity contours are extremely localized with green and yellow zones engulfing the peak velocity red spots. Generally, very low velocities are computed throughout the *mass of the composite elevator* material, indicating that very weak percolation of water occurs. The momentum of the entering flow is insufficient to stimulate significant mass transfer in the elevator matrix. When the inlet velocity is quadrupled to 20 m/s (Fig. 15), the original velocity contours are accentuated. The red peak zones expand and the green and yellow zones (slightly lower velocity) spread outwards in a cross-like configuration, whereas at $V = 5$ m/s they appear in diamond configurations. Sharper zones of higher velocity are also stretched laterally along the leading-edge direction. With the maximum entry velocity (100m/s) as shown

in Fig. 16, the cross patterns (green/yellow relatively high velocity magnitudes) are further elongated and extend deeper towards the central zone of the elevator. They are also amplified and becoming more strongly aligned to both the leading edge and trailing edge. The central zone also features a growth in velocity (lighter green zones) but again these are confined to the central zone of the elevator and do not migrate towards the elevator tip or opposite boundary. Clearly the *moisture penetrates a substantially larger proportion of the upper surface of the elevator with increasing inlet velocity at the fastener holes*. The higher inlet velocity approaches real flight conditions and therefore it is apparent that such scenarios will require better ground inspection, maintenance and stricter quality regulations to ensure that fasteners are not loosened or compromised. There is potentially the possibility of structural degradation and material damage associated with weakening of the composite in the proximity of the fastener holes. These are of great concern in practical operations and rapid attention is recommended on a regular basis by ground maintenance crews.

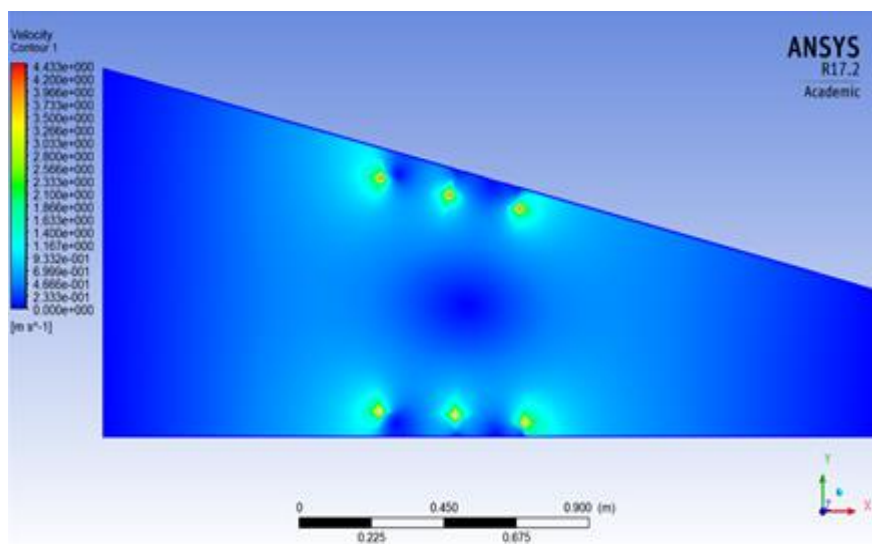


Fig. 14: 6 affected fastener holes - top surface – velocity contour $V = 5$ m/s

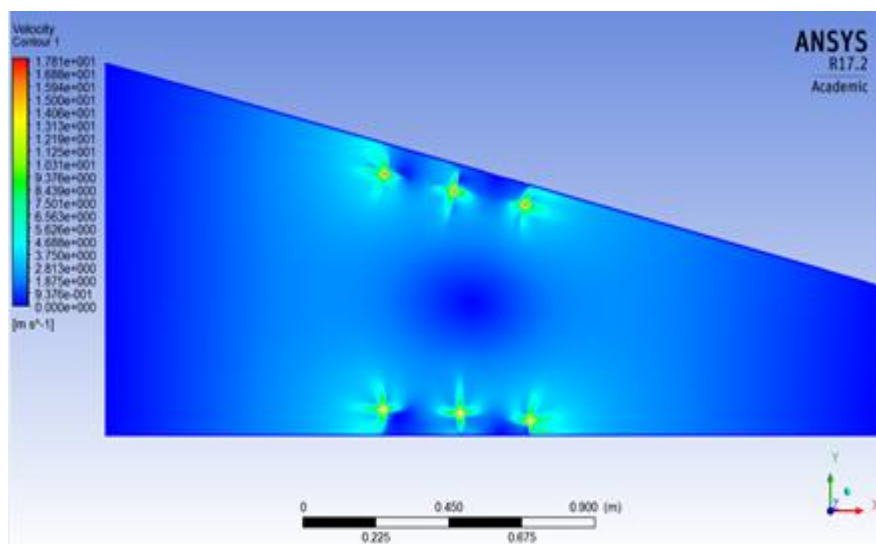


Fig. 15: 6 affected fastener holes - top surface – velocity contour $V = 20$ m/s

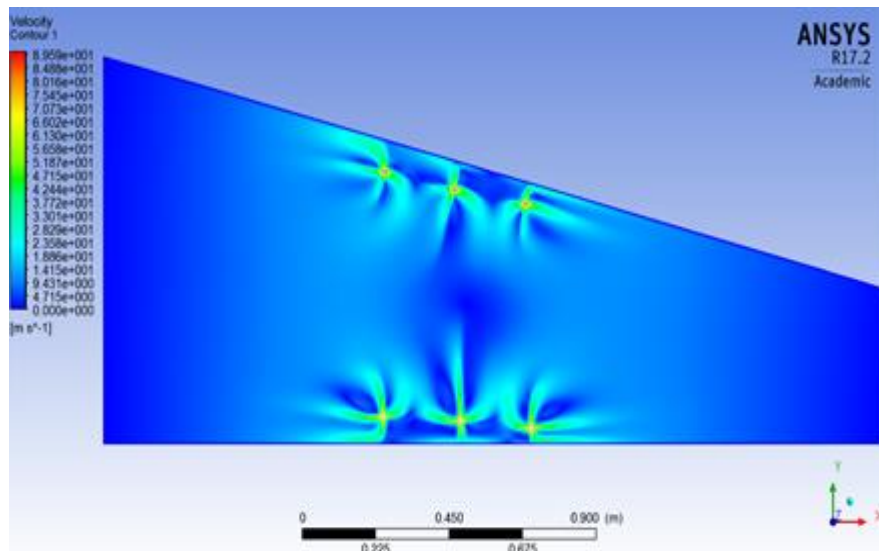


Fig. 16: 6 affected fastener holes - top surface – velocity contour $V = 100$ m/s

5.3 Effects of voids

Figs. 17-19 illustrate the influence of random void distribution on the pressure, velocity and streamline contours, through the mass of the elevator, as a model of manufacturing defects within the elevator composite. Voids are material defects in the manufacture of any aircraft composite wing. They are inevitable features despite very precise manufacturing techniques. They arise invariably and can become worse with aircraft flight hours where they may expand or propagate uncontrollably through a wing section and elevator section. They allow water to ingress into the composite. To simplify the simulation, we assume that the voids are homogeneously distributed rather than heterogeneously i.e. the voids are selected to be of the same size. Fig. 17 shows that the moisture having penetrated the elevator surface and deep into the body of the material attains highest magnitudes at the trailing edge. The lower volume of material available here results in greater pressures. Very low pressures are computed at the leading edge where a greater volume of material is present. The presence of voids has a reduced effect here. There is a smooth transition in fluid pressure from the leading edge to the trailing edge. Fig. 18 indicates that the presence of voids near the trailing edge where the area decreases results in lower velocity magnitudes. However, there are zones of higher velocity further into the elevator away from the trailing edge. Large velocity clusters are also computed near the upper surface at the leading edge, although they are smaller than those witnessed in the last third chord zone section of the elevator. Fig. 19 visualizes the flow paths from the inlet holes towards the voids. Generally, as expected, the flow paths are tortuous and severely distorted as we progress away from the voids. The velocity streamlines depict the moisture pathways *through and around the embedded voids* and clearly disperse in all directions, with no bias to any specific direction, in the structure. Maximum intensity is computed towards the trailing edge indicating that circulation here is strongest. Generally weak circulation is observed in the leading-edge vicinity. Voids near the trailing edge are more likely to affect the materials properties compared with voids located towards the leading edge. This is probably due to the decreasing cross-sectional area at the trailing edge where the moisture can easily get trapped, generating the highest-pressure concentration at the elevator tip. However higher velocity contours are also generated close to this zone. Therefore, fabrication of the elevator requires great consideration and *satisfactory design at the trailing edge* to avoid voids and/or microcracks at smaller cross-sectional areas of the aerofoil.

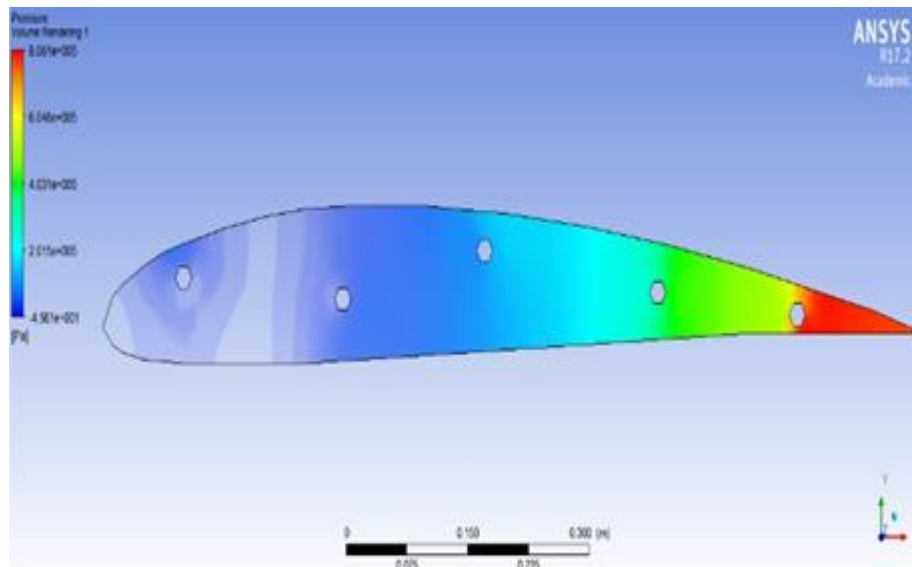


Fig. 17: Total Pressure contour - Random voids in AS4-3k

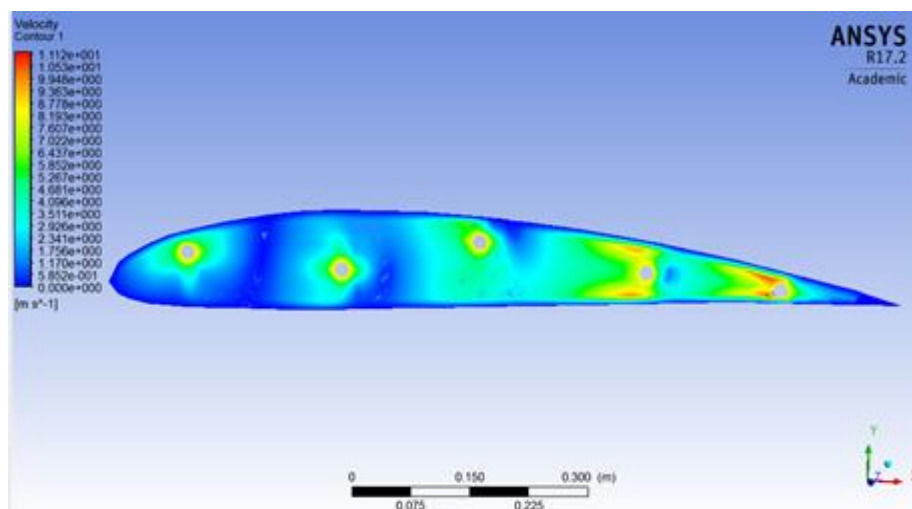


Fig. 18: Velocity contour - Random voids in AS4-3k

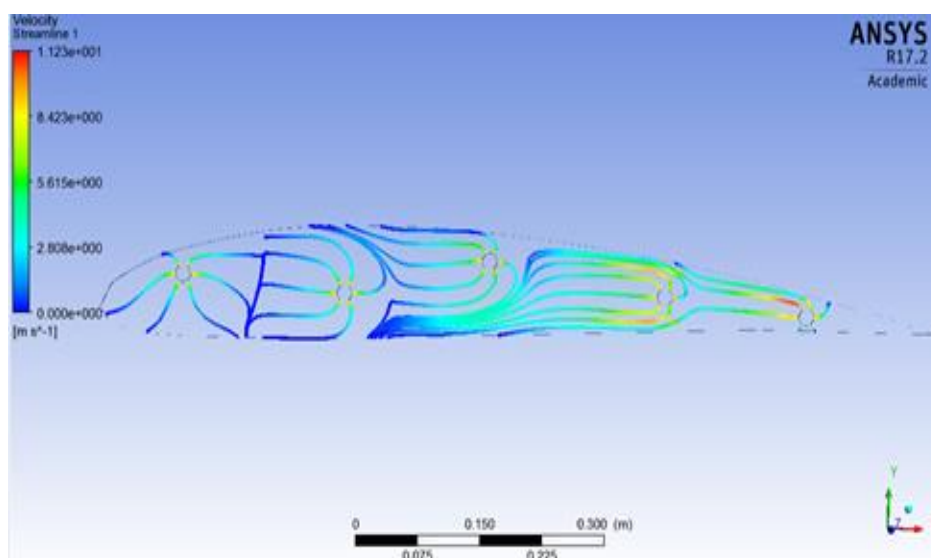


Fig. 19: Velocity Streamline - Random voids in AS4-3k

5.4 Effects of voids of different dimensions

Figs. 20-22 illustrate the influence of voids of different dimensions on respectively velocity distribution, X-velocity contours and pressure contours. Considering fig. 22 first, comparing with the plot computed in fig. 19, it is evident that a simple modification in dimensions (larger and smaller voids, rather than equal sized voids) considerably modifies the pressure variation through the elevator. The smooth transition computed in fig. 19 is now replaced with random zones of low pressure interspersed through the elevator cross-sectional area with greater magnitudes between these zones and maximum values at the inlet holes. The larger void towards the leading-edge results in enhanced moisture dispersion and lower values towards the smaller void near the trailing edge. Fig. 20 shows that the highest velocity i.e. greatest acceleration of water flow is always at the inlets. The larger void towards the trailing edge leads to stronger dispersion. Fig. 21 shows that there are however zones of high X-velocity at the lower surface of the elevator also and several similar zones near the upper surface and lower surface towards the trailing edge. However, these “accelerated clusters” are eliminated at the elevator tip (trailing edge) itself.

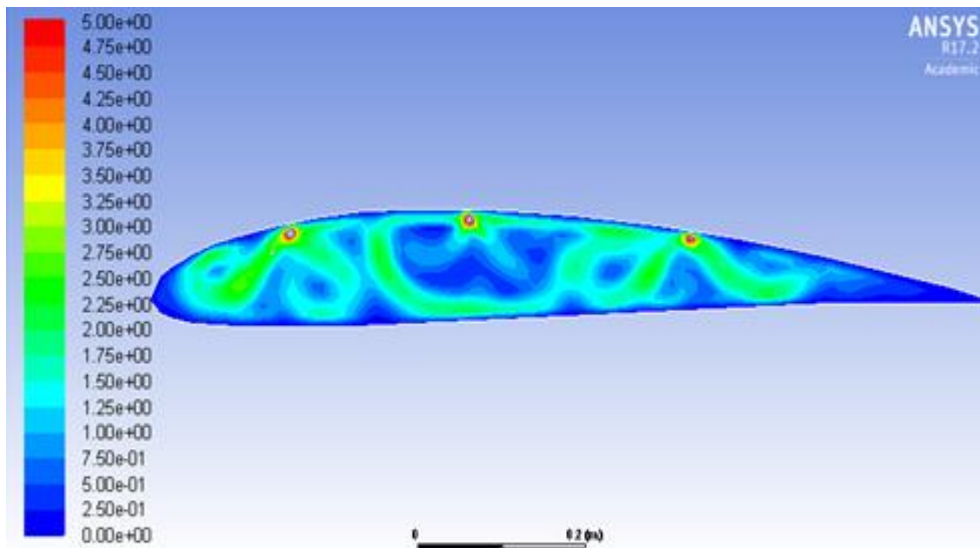


Fig. 20: Velocity Contour - Random voids of different sizes in AS4-3k

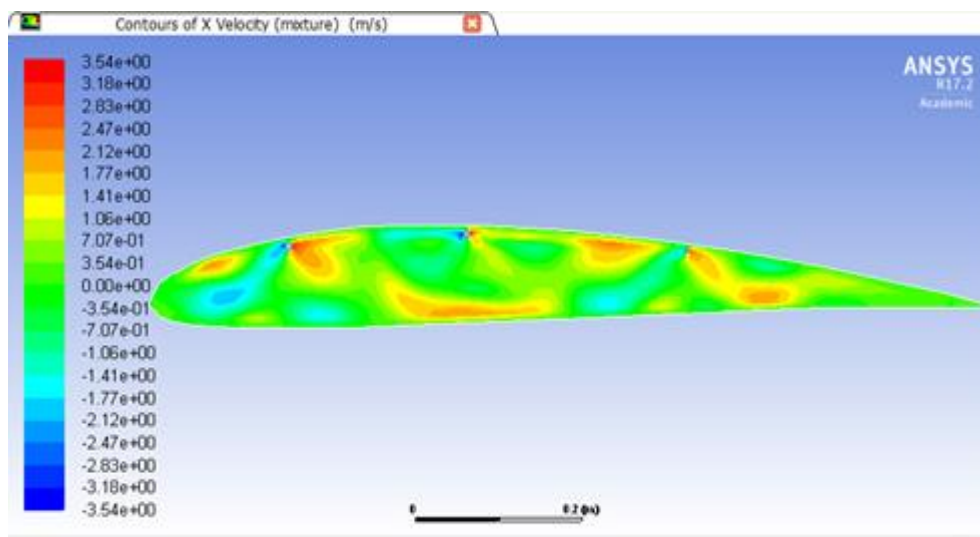


Fig. 21: X-Velocity Contour - Random voids of different sizes in AS4-3k

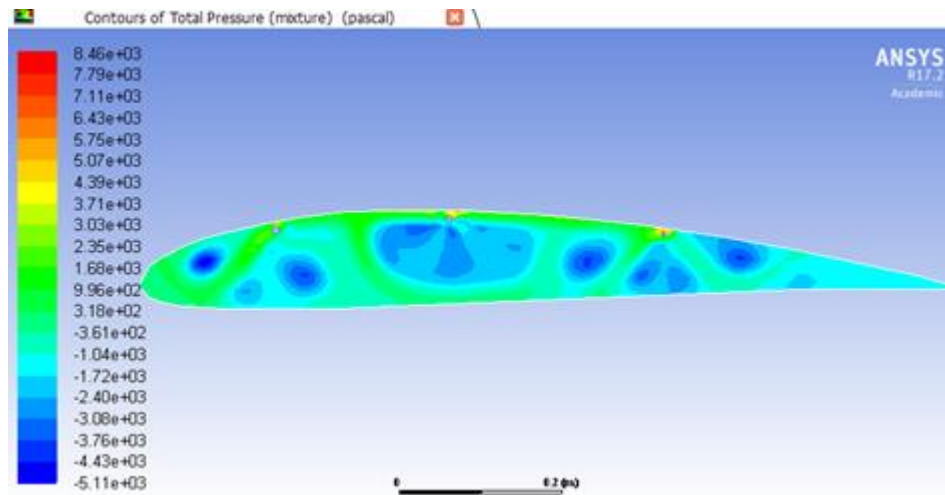


Fig. 22: X-Velocity Contour - Random voids of different sizes in AS4-3k

5.5 Effects of water ingress in the whole elevator

Figs. 23-26 present the three-dimensional CFX simulations for the impact of water ingress on the entire elevator, including several FSI (fluid structure interaction) simulations. It is important to appreciate that the elevator is a very key aerodynamic feature of any aircraft. Both a *horizontal stabilizer* and an *elevator* feature at the rear of the fuselage of most aircraft. The elevator is the small moving section at the rear of the stabilizer that is attached to the fixed sections by hinges. The surface of the elevator is extremely important in aerodynamic control since as the elevator moves, it varies the amount of force generated by the tail surface and is used to generate and control the pitching motion of the aircraft. There is an elevator attached to each side of the fuselage. The elevators work in pairs; when the right elevator goes up, the left elevator also goes up. The elevator surface is also critical in controlling the position of the nose of the aircraft and the angle of attack of the wing. Changing the inclination of the wing to the local flight path changes the amount of lift which the wing generates. This, in turn, causes the aircraft to climb or dive. During take-off the elevators are used to bring the nose of the aircraft up to begin the climb out. During a banked turn, elevator inputs can increase the lift and cause a tighter turn and the elevator surface is vital therefore for safe commercial (and also military) aircraft motions. The elevator surface works by changing the effective shape of the airfoil of the horizontal stabilizer. Changing the angle of deflection at the rear of the airfoil changes the amount of lift generated by the foil. With greater downward deflection of the trailing edge, lift increases. With greater upward deflection of the trailing edge, lift decreases and can even become negative. Overall therefore it is vital to ensure that the elevator performs aerodynamically efficiently and is not damaged by water ingress. Fig. 23 shows that moisture is dispersing from the inlets to the leading and trailing edges which both exhibit higher pressures (red zones). With four fastener holes the highest pressure is computed at the upper surface of the elevator near the trailing edge, confirming the ANSYS FLUENT findings described earlier. There are also high-pressure zones at the chord section especially near both the trailing edge and leading edge and this is *not visualized* in the two-dimensional ANSYS FLUENT simulations. The elevator surface generally shows lesser pressure build up relative to the boundaries (trailing and leading edges). Fig. 24 depicts the velocity contour evolution at an inlet speed of 4.553 m/s. The only substantial acceleration is computed around the inlets, with greater magnitudes and larger zones of high velocity near the trailing edge. The remainder of the elevator body does not experience any marked velocity escalation. FSI (fluid structure interaction) analyses are

shown in figures 25 and 26, computed at 100s. Fig. 25 shows that when structural interaction with the influx of water is included, *high deformations are computed at the trailing edge*. Elsewhere there is no significant deformation in the elevator, reinforcing the earlier suggestions that ground maintenance crews are required to focus attention on the elevator tip region which is most potently affected by water ingress. Fig. 26 shows that low normal (direct) stress magnitudes are computed generally on the elevator surface (for 4 fastener holes) except for the trailing and leading-edge regions (near the inlets) where stress peaks are observed. These high stress zones (red regions) are pronounced at the trailing edge. Highest pressure is generated via water penetration at the trailing edge due to the smallest cross-sectional area. Although some insight is provided via FSI (fluid structure interaction), more refinement in material specification is needed with other combinations. Furthermore, *interfacial sliding* of the fluid and structural mesh may lead to better simulation results as elaborated by Bathe et al. [35]. FSI (fluid structure interaction) capabilities are limited in the ANSYS FLUENT-structural suite.

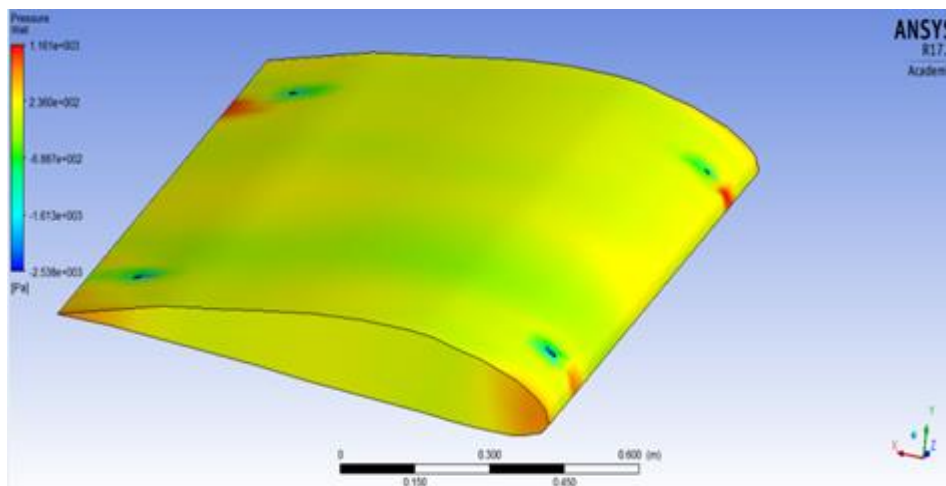


Fig. 23: 3D AS4 elevator study – CFX – 4 affected fasteners – Pressure contour

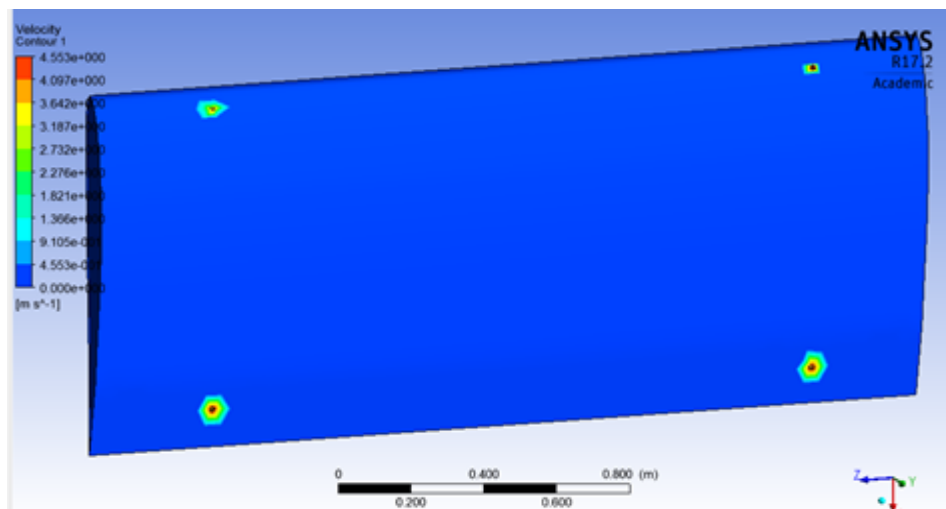


Fig. 24: 3D AS4 elevator study – CFX – 4 affected fasteners – Velocity contour

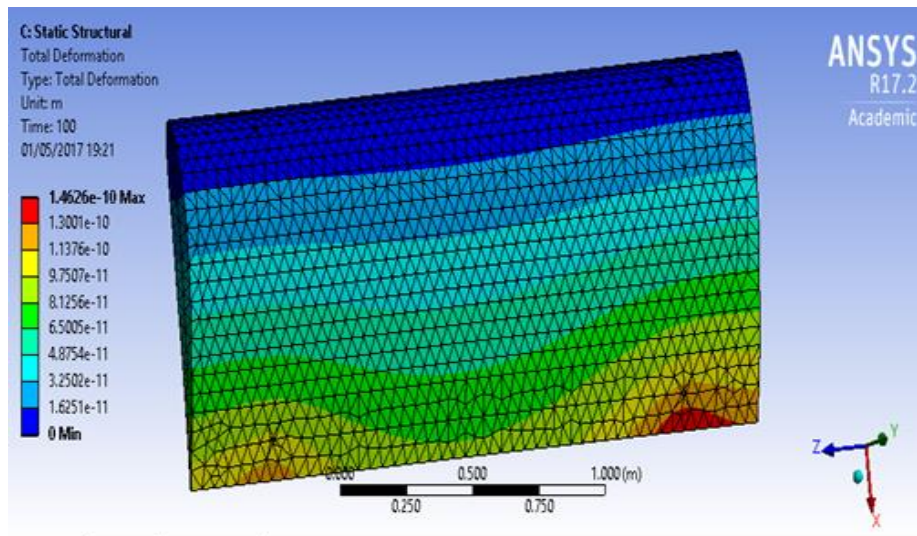


Fig. 25: 3D AS4 elevator study – FSI – 4 affected fasteners – Total Deformation

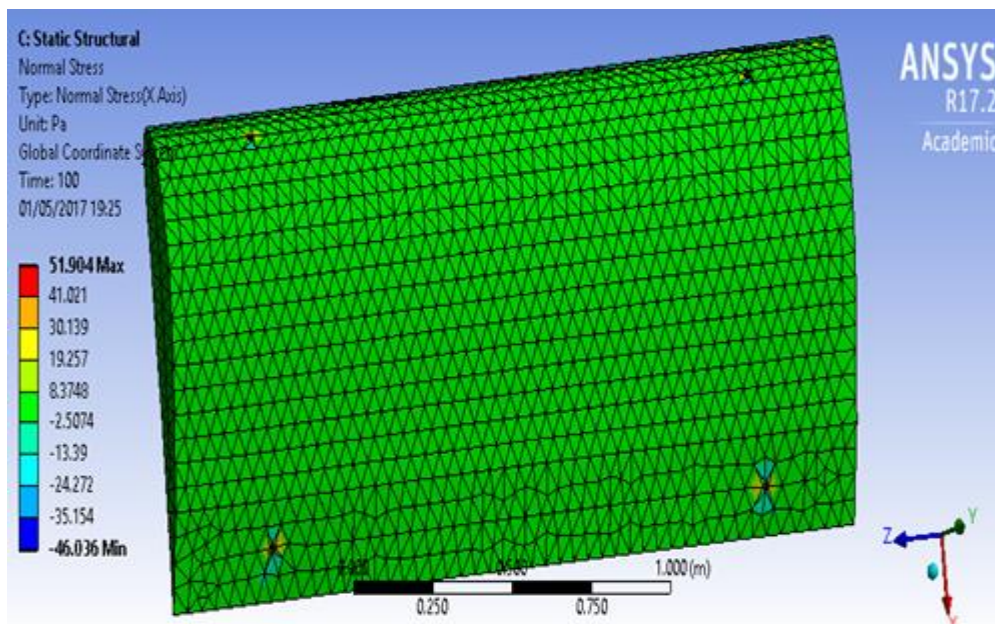


Fig. 26: 3D AS4 elevator study – FSI – 4 affected fasteners – Normal Stress

5.6 Comparisons between composite materials: AS4-3k / CFRP Epoxy / Kevlar

Finally, **Figs. 27a-f** illustrate the 3-dimensional pressure and velocity contours for various composite materials (AS4-3k / Carbon Fiber Reinforced Polymers (CFRP) Epoxy / Kevlar) computed with CFX. Here figs. 27a-c correspond to the pressure contours and figs. 27 d-f to the velocity contours. CFX 3-dimensional analysis enables comparison between different materials in order to study the varied response of AS4-3k, Epoxy Carbon Fiber Reinforced Polymers (CFRP) and Kevlar CFRP, common aerospace composite materials employed in commercial airliner structures. AS4-3k is widely used in aviation and other sectors including marine and civil engineering. Epoxy Carbon Fiber Reinforced Polymer (CFRP) is the most commonly used material for elevators and is therefore particularly relevant to the current study. The pressure contours of the 3D elevators made with each material shows that AS4-3k is the weakest amongst the other two being simulated under identical conditions. Indeed, the pressure is much more significant for the AS4 material with moisture concentration at both leading and trailing edges, which are locations difficult to inspect and remedy in the event of damage. Both Carbon Fiber

Reinforced Polymer (CFRP) epoxy and Kevlar Carbon Fiber Reinforced Polymer (Kevlar CFRP) show almost negligible pressure on the whole elevator. The velocity plots are however very similar. The maximum velocity is observed at the inlets although different magnitudes are computed for the three different composite cases, with the best response achieved with epoxy Carbon Fiber Reinforced Polymer (CFRP).

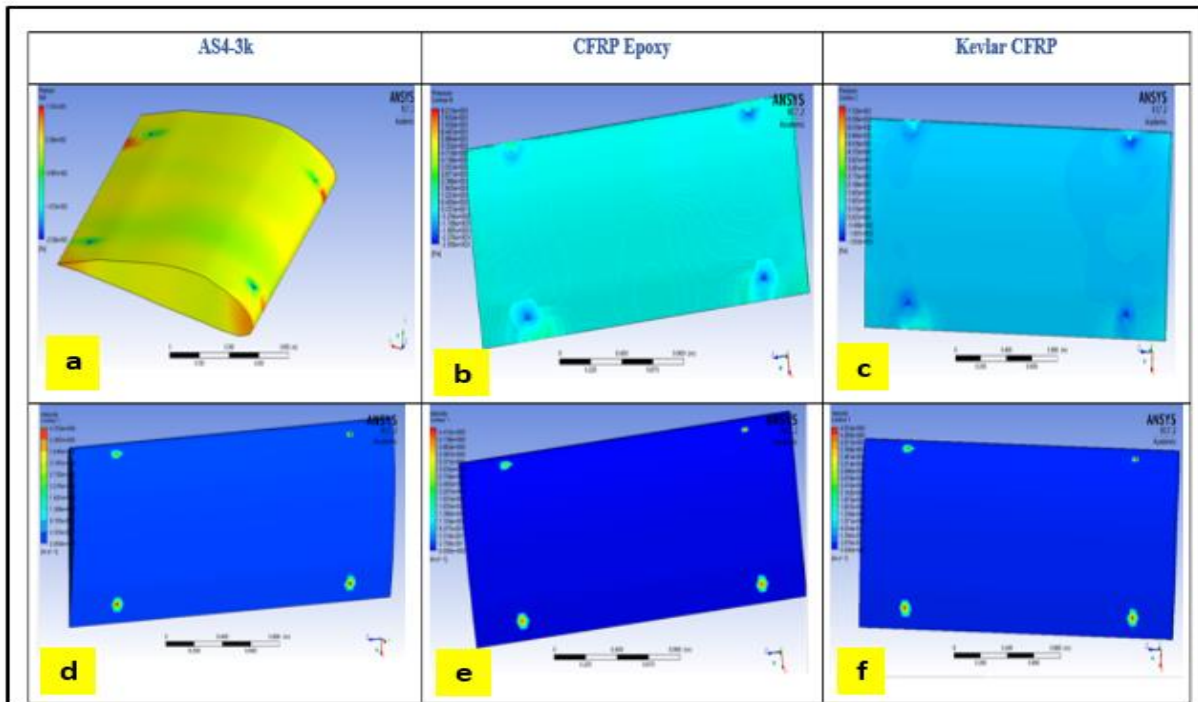


Fig. 27 a-f: Pressure and Velocity Contours for various composite materials – CFX

6. CONCLUSIONS

Computational fluid dynamic and fluid-structure interaction simulations have been conducted to investigate the water ingress mechanisms and effects on elevator aircraft structural behaviour. ANSYS FLUENT and CFX commercial finite volume codes have been employed. Both two-dimensional (ANSYS FLUENT) and three-dimensional (CFX) analyses have been described. The influence of different numbers of water inlet holes, voids and void dimensions within the composite and water ingress velocity on pressure, velocity and streamline distributions has been computed. Three-dimensional CFX FSI (fluid structure interaction) analysis has also been conducted to yield total deformation and normal stress plots for the case of four fastener holes. ANSYS FLUENT is shown to generate good basic results that are sufficient for elementary assessment. However, discrepancies have been observed in the CFX solver, which does not provide accurate answers with finer meshes. FSI (fluid structure interaction) is also seen, not to take into account the material properties of the composite simulated. The ANSYS FLUENT solver is seen to achieve acceptable and satisfactory solutions for velocity and pressure distributions, specifically for two-dimensional simulations which provide a fast-inexpensive alternative to long-term, real time experimental studies. CFX provides good three-dimensional simulation capabilities. A comparison between commonly used materials in commercial aero-structures was conducted through CFX which indicated that negligible moisture is present in the epoxy resin Carbon Fiber Reinforced Polymer (CFRP) which is the most popular composite for aircraft elevators, whereas significant water ingress is computed for AS4 composites. This confirms the choice of industry of using epoxy Carbon Fiber Reinforced Polymer (CFRP). Further analysis is

warranted, and other software may provide better FSI (fluid structure interaction) accuracy, for example the excellent multi-physics code, ADINA [36]. Computational Fluid Dynamics (CFD) can however be used to implement possible mitigation pathways and furthermore is the most practical strategy for corroboration of experimental testing available to engineers. Although not considered in the current work, a promising concept for mitigating water ingress could be the implementation of *thin hydrophobic films* [37] on the outer ply of a composite structure. These bio-engineered materials repel water and therefore oppose water ingress into the composite wing structure. Hydrophobic films [38] have been shown to significantly improve the mechanical properties by reducing water ingress and the intrusion of other aviation fluids (hydraulic oils such as Skydrol). Glass composite components with hydrophobic films showed about 50 % higher strength in the hydraulic fluid compared to components without any barrier film. However, these coating materials are still under development and their adhesive stability and durability would be critical to successful implementation. Another solution to water ingress is coating wing structures with Teflon [39] which is a hydrophobic fluoropolymer resin, which has the added advantages high tensile strength, prolonged fatigue life and weather-resistance. These could be possibly simulated with non-Newtonian flow models [40]. Other mitigations pathways exist. Simulations could consider micro-cracking that could be thermally or mechanically induced, thus providing a pathway for moisture and a solution could be to toughen the additive in the matrix or modify the size of the fibre. The porosity in the sandwich faces can be successfully mitigated by increasing the resin content or also, the thickness of the component, although these are very challenging to analyse computationally. Adding an extra layer of adhesive film creates a better seal preventing moisture ingress. Increasing the toughness of composite face sheets is yet another solution to increase the fracture toughness of the assembly noting that impact-damaged face sheets may go undetected for long periods of time, due to the lack of visible damage. Overall the water ingress composite structure problem is still under active investigation. Many simulation techniques can be explored to better simulate the intricate mechanisms of water migration and real-time effects on structural integrity during actual in-flight conditions. Possibly a multi-scale approach, which couples internal mechanical states in the deformable composite matrix with Fick's mass diffusion which can predict swelling, relaxation, brittle fracture and other complex phenomena [41] would be best analyzed with *molecular dynamics* codes which require very high-powered hardware. These are currently being explored. The results of these analyses will be communicated imminently.

ACKNOWLEDGEMENTS

This research did not receive any specific grant from funding agencies in the public, commercial, or not-for-profit sectors.

COMPLIANCE WITH ETHICAL STANDARDS:

The ethical standards are considered in writing this paper. The authors have no conflict of interest with anybody or any organizations/companies.

REFERENCES

- [1] Anderson, J.P., Altan, M.C.: Voids in composites with continuous fibre reinforcement. *Society of Plastic Engineers - Plastics Research Online.*, (2014). <https://doi.org/10.2417/spepro.005487>.
- [2] Hayes, B.S., Gammon, L.M., (Eds): *Optical Microscopy of Fiber-Reinforced Composites*. ASM Int. USA (2010).

- [3] Wong, K.J., Tamin, M.N.: Non-Fickian moisture uptake characterization of epoxy-based moulding compounds with thickness effect. *36th Int Elect Manufacturing Tech Conf.* November 11 – 13, Johor, Malaysia (2014).
- [4] Mazor, A., Broutman, L.J., Eckstein, B.H.: Effect of long-term water exposure on properties of carbon and graphite fiber reinforced epoxies. *Polymer Eng. Sci.* 18(5), 341-349 (1978).
- [5] Marom G., Broutman, L.J.: Moisture penetration into composites under external stress. *Polymer Composites.* 2(3),132–136 (1981). <https://doi.org/10.1002/pc.750020310>.
- [6] Jackson, W.C., O'Brien, T.K.: Water intrusion in thin-skinned composite honeycomb sandwich structures. *J. American Helicopter Soc.* 35(4), 31-37 (1988).
- [7] Komai, K., Shiroshita, S., Kilidjian, G.: Influence of water on mechanical properties and fracture mechanisms of CFRP/aramid honeycomb core sandwich beams. *J. Japan Soc. Mater. Sci.* 44(505), 1273–1278 (1995).
- [8] Cise, D., Lakes, R.: Moisture ingress in honeycomb core sandwich panels: directional aspects. *J Compos Mater.* 31(22), 2249–2263 (1997).
- [9] LaPlante, G.: Detection of water ingress in composite sandwich structures: a magnetic resonance approach. *NDT & E Int.* 38, 501-507 (2005).
- [10] Crawley, N.M.: Non-destructive testing and the link between environmental degradation & mechanical properties of composite honeycomb panels. *Proc. American Helicopter Soc. 62nd Annual Forum, Phoenix, Arizona, USA, May 9-11* (2006).
- [11] Li, C., Ueno, R., Lefebvre, V.: Investigation of moisture ingress and migration mechanisms of an aircraft rudder composites sandwich structure, *38th International Society Advancement Manufacturing and Process Engineering (SAMPE) Technical Conference, Dallas, November* (2006).
- [12] Arici, A.A.: Effect of hygrothermal aging on polyetherimide composites. *J. Reinforced Plastics and Composites.* 26, 1937-1942 (2007).
- [13] Youssef, G., Fréour, S., Jacquemin, F.: Stress-dependent moisture diffusion in composite materials. *J. Compos Mat.* 43(15),1621–1637 (2009).
- [14] Dana, H.R., Perronnet, A., Fréour, S., Casari, P., Jacquemin, F.: Identification of moisture diffusion parameters in organic matrix composites. *J. Compos. Mat.* 47, 1081-1092 (2013).
- [15] Chateauminois, A., Vicent, L., Chabert, B., Soulier, J.P.: Study of the interfacial degradation of a glass-epoxy composite during hygrothermal ageing using water diffusion measurements and dynamic mechanical thermal analysis, *Polymer.* 35(22), 4766-4774 (1994).
- [16] Costa, M.L.: Effect of void content on the mechanical properties on the carbon fiber/epoxy and carbon fiber/bismaleimide advanced composites. *PhD Thesis, Instituto Tecnológico de Aeronáutica: ITA, São José dos Campos, SP, Brazil* (2002).
- [17] Ibarra-Castanedo, C., Marcotte, F., Genest, M., Brault, L., Farley, V., Maldague, X.P.V.: Detection and characterization of water ingress in honeycomb structures by passive and active infrared thermography using a high-resolution camera, *11th International Conference on Quantitative InfraRed Thermography,* 11-14 June, Naples Italy (2012).
- [18] Pan, C., Hilpert, M.: Lattice-Boltzmann simulation of two-phase flow in porous media. *Water Resources Research.* 40, 1-20 (2004).

- [19] Han, B.G., Guliaev, A.B., Walian, P.J., Jap, B.K.: Water transport in AQP0 aquaporin: molecular dynamics studies. *J. Molecular Biol.* 360, 285-296 (2006).
- [20] Anwar Bég, O., Zueco, J., Bhargava, R., Takhar, H.S.: Magneto-hydrodynamic convection flow from a sphere to a non-Darcian porous medium with heat generation or absorption effects: network simulation. *Int. J. Thermal Sci.* 48(5), 913-921 (2009).
- [21] Ionita, A.: A model for fluid ingress in closed cell polymeric foams. *Mech. Mat.* 39, 434-444 (2007).
- [22] Gueribiz, D., Jacquemin, F., Fréour, S.: A moisture diffusion coupled model for composite materials. *Euro. J. Mech- A/Solids.* 42, 81-89 (2013).
- [23] Telford, R., Katnam, K.B., Young, T.M.: The effect of moisture ingress on through-thickness residual stresses in unsymmetric composite laminates: A combined experimental–numerical analysis. *Composite Struct.* 107, 502-511 (2014).
- [24] Vavilov, V.P., Pan, Y., Moskovchenko, A.I., Čapka, A.: Modelling, detecting and evaluating water ingress in aviation honeycomb panels. *Quantitative InfraRed Thermography J.* 14, 1-12 (2017).
- [25] Adler, P.: *Porous Media: Geometry and Transport*. Butterworths, Chemical Engineering Series, USA (1992).
- [26] *ANSYS FLUENT 17.1 User Manual*.: Swanson Analysis Systems, Pennsylvania, USA (2016).
- [27] *ANSYS CFX User Manual*.: Swanson Analysis Systems, Pennsylvania, USA (2016).
- [28] *The Composite Materials Handbook*.: US Department of Defence, Aberdeen, Maryland, USA (2002).
- [29] Islam, B.: Water Ingress in Composite Materials, *BEng (Hons) Aeronautical Engineering Project Report. Aeronautical and Mechanical Engineering, May, University of Salford, Manchester* (2017).
- [30] Daud, H.A., Li, Q., Anwar Bég, O., AbdulGhani, S.A.A.: Numerical investigations of wall-bounded turbulence. *Proc. Inst. Mech. Eng-Part C: J. Mech. Eng. Sci.* 225, 1163-1174 (2011).
- [31] Daud, H.A., Li, Q., Anwar Bég, O., AbdulGhani, S.A.A.: CFD modeling of blowing ratio effects on 3-D skewed gas turbine film cooling. *11th Int. Conf. Advanced Computational Methods and Experimental Measurements in Heat Transfer, 14-16 July, Tallinn, Estonia* (2010).
- [32] Daud, H.A., Li, Q., Anwar Bég, O., AbdulGhani, S.A.A.: Numerical study of flat plate film cooling effectiveness with different material properties and hole arrangements, *12th UK National Heat Transfer Conference 30th August- 1st September, School of Process Engineering, University of Leeds, UK* (2011).
- [33] Sze, C.N.P., Hughes, B.R., Anwar Bég, O.: Computational study of improving the efficiency of photovoltaic panels in the UAE. *ICFDT 2011-International Conference on Fluid Dynamics and Thermodynamics January 25-27, , Dubai, United Arab Emirates* (2011).
- [34] El Gendy, M., Anwar Bég, O., Kadir, A., Islam, M.N., Tripathi, D., B. Vasu: ANSYS CFX/FLUENT Computational fluid dynamics simulation and visualization of Newtonian and non-Newtonian transport in a peristaltic micro-pump. (2019). *Under review*.
- [35] Bathe, K.J., Zhang, H., Ji, S.: Finite element analysis of fluid flows fully coupled with structural interactions. *Comput & Struct.* 72, 1–16 (1999).
- [36] Wang, X., Gordnier, R., Ji, S., Bathe, K.J.: A Study of 2D+ Airfoil FSI Models with Different FSI Approaches, *Proc. 50th AIAA/ASME/ASCE/AHS/ASC Structures. Structural Dynamics, and Materials Conference, AIAA 2009-2573* (2009).

- [37] Morita, K., Okamoto, K., Aoki, A., Kimura, S., Sakaue, H.: Hydrophobic Coating Study for Anti-icing Aircraft. *SAE Technical Paper*. 38, 0010 (2011). <https://doi.org/10.4271/2011-38-0010>.
- [38] Kececi, E., Asmatulu, R.: Effects of moisture ingress on polymeric laminate composites and its prevention via highly robust barrier films. *Int. J. Adv. Manuf. Tech.* 73, 1657-1664 (2014).
- [39] Blumm, J., Lindemann, A., Meyer, M., Strasser, C.: Characterization of PTFE Using Advanced Thermal Analysis Technique. *Int. J. Thermophys.* 40, 13-14 (2011).
- [40] Rana, S., Mehmood, R., Satya Narayana, P.V., Akbar, N.S.: Free convective nonaligned non-Newtonian flow with non-linear thermal radiation. *Commun. Theor. Phys.* 66, 687–693 (2016).
- [41] Koo, B., Subramanian, N., Chattopadhyay, A.: Molecular dynamics study of brittle fracture in epoxy-based thermoset polymer. *Composites Part B: Eng.* 95, 433-439 (2016).

